single slide experiment, using the ratio of means formula (F635 Mean−B635Median/F532 Mean−B532 Median) according to GenePix Pro. 4.0. The standard deviation of each clone was calculated. We regarded the signal ratio as "abnormal" if it ranged out of ±3 SD in both CGH1 and CGH2 based on data of the study using the normal control and the positive control [46,XX,inv dup del(8)(qter → p23.1:: p23.1 → p11.23:)], and used the criterion for further FISH analyses (Fig. 1A).

RESULTS

We analyzed 30 idiopathic MR patients and found a total of 66 clones indicating genomic dosage changes (12 deletions and 54 duplications) in 25 cases (Figs. 1B and 2). Of the 30 MR patients, 5 (17%) had submicroscopic chromosome abnormalities (Table I), including 2 interstitial deletions (MR88 and MR126), a terminal deletion (MR96), an interstitial duplication (MR135), and an unbalanced reciprocal translocation (MR118). The unbalanced

Fig. 1. Results of BAC array CGH. A: Hybridization of normal control male DNA (Cy3) and another normal control male DNA (Cy5) (upper panel), and normal control female DNA (Cy5) and DNA of 46,XX, inv dup del(8)(qter → p23.1::p23.1 → p11.23:) (Cy3) (lower). Cy5/Cy3 ratios are indicated. Ratios of clones mapped to chromosomal 8p are shown. Note that ratios of deleted or duplicated clones range outside ±3 SD from the mean. B: Hybridization of MR135 DNA (Cy3) and normal control female DNA (Cy5). Ratios of all chromosome-21 clones are displayed. Two clones were found duplicated (RP11-316L10 and RP11-90N6). Each clone's ratio was shown as two dots because it was spotted twice in the array.

segments in the five patients ranged in size from 0.7 to 9.1 Mb. G-banded chromosomal analysis (550-band level) could afterward confirm subtle changes in MR96 and MR118 (Fig. 3A) but failed to identify the aberrations in MR88, MR126, and MR135 (data not shown).

46XY, del(15)(q11.2q12)mat in MR88

BAC aCGH detected deletion at RP11−171C8 in MR88. RP11−171C8 corresponds to the *UBE3A* gene that is paternally imprinted. This deletion was also identified in his mother and his maternal grandfather. Maternal deletion of *UBE3A* leads to Angelman syndrome (AS, OMIM #105830). MR88 was diagnosed as AS retrospectively, as presenting with severe MR, epilepsy, ataxic gait, happy disposition, characteristic facial features, and disrupted sleep (Table I). Paternal *UBE3A* deletion in the healthy mother did not cause any abnormal symptoms.

46,XX,del(1)(1q43) in MR96

The deletion spanning the 9.1-Mb genomic region from RP11−201D24 to RP11−152M6 was confirmed (UCSC coordinates, chromosome 1 nucleotide 235232983−244275234). As her parental samples were unavailable, it remains unanswered as to whether this deletion truly causes MR. However, in the literature, a similar deletion, del(1)(q43qter) showed a consistent pattern of anomalies including heart defects, agenesis of the corpus callosum, and cleft palate as well as MR [Schinzel, 2001], suggesting that the deletion may contribute to MR in the patient. Intrauterine growth retardation, growth abnormalities, and dysmorphic facial features were also recognized (Table I), but detailed clinical information was not available in this patient.

46XY,der(22)t(19;22)(p13.3;q13.31)pat in MR118

An unbalanced chromosomal translocation was identified in MR118 (Fig. 3B), which was derived from the father who possessed a balanced translocation, t(19;22)(p13.3;q13.31) (Fig. 3C). The remarkable phenotype is female (Table I). Normal male sex chromosomes (XY) and normal *SRY* sequence were confirmed in this patient (data not shown).

The trisomic region at 19p13.3 is almost 6 Mb in size (UCSC coordinates, chromosome 19 nucleotide 1−5893448). In reported patients presenting with dup(19)(pterp13.2), growth retardation, developmental delay, hyper muscle tonus, deafness, heart anomaly, and hydronephrosis have been recognized, but sex reversal has never been described [Schinzel, 2001].

The deleted region at 22q13.31 was almost 3 Mb in size (UCSC coordinates, chromosome 22 nucleotide 46600003−49554710). A total of eight patients with
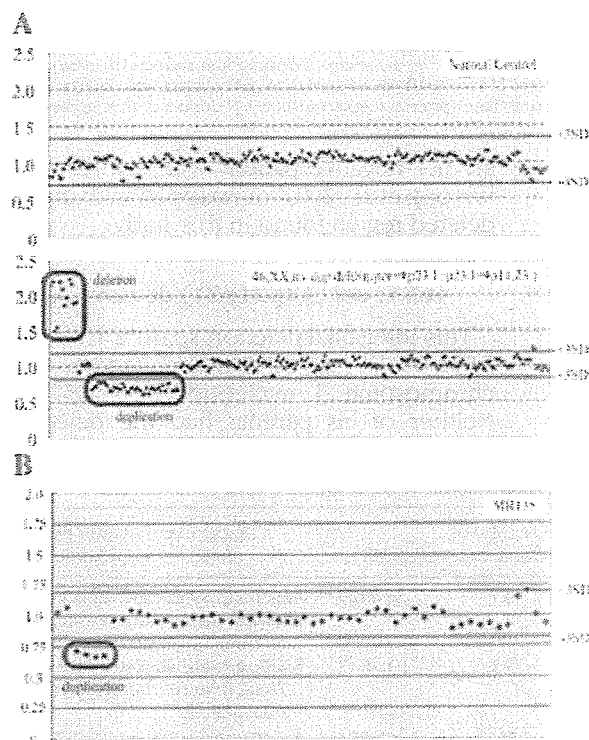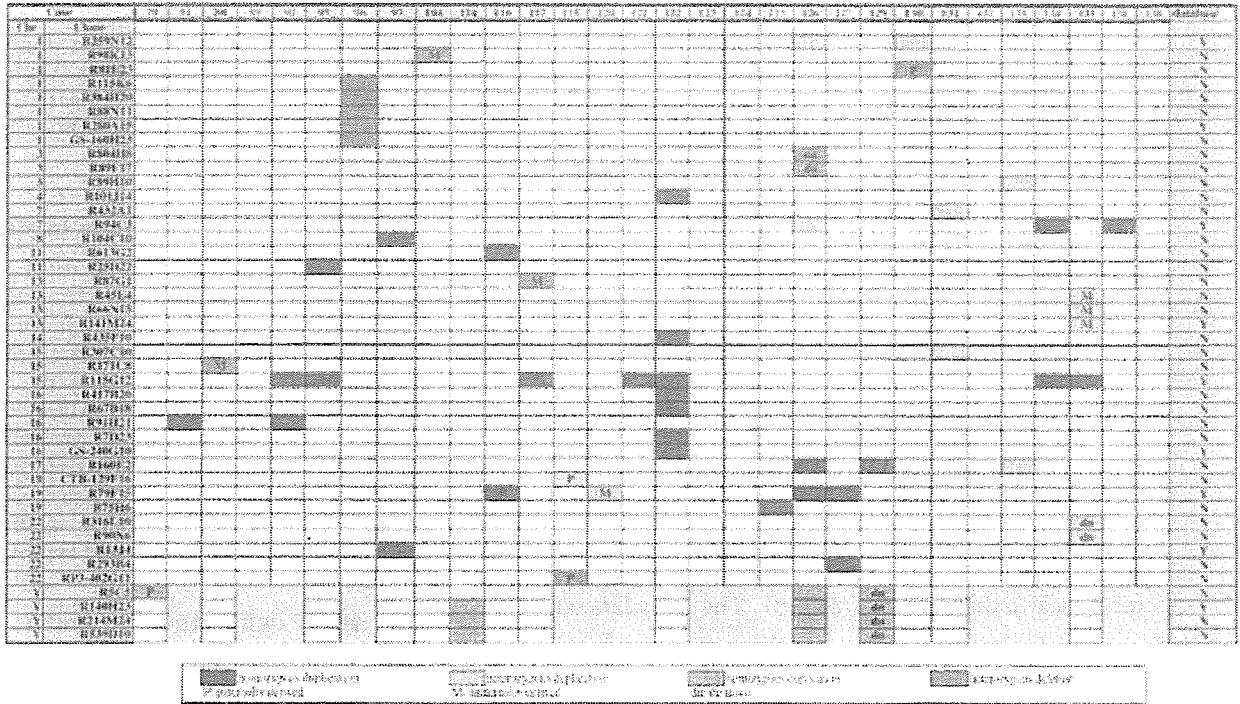
Fig. 2. Summary of BAC array CGH and FISH studies on MR patients. Top yellow row indicates MR patients (male in black, and female in red). Left green columns show information of clone IDs and their chromosomes. Duplications are shown as in red (homozygous), orange (heterozygous), and pink (hemizygous). Heterozygous deletions are in sky blue. Parental origin of changes is indicated as P (paternal) and M (maternal); dn, de novo. Y in right column (pale blue) indicates clone/locus registered as copy number polymorphism (CPN) in the Database of Genomic Variants (http://projects.tcag.ca/variation/). N clone/locus not registered in the database.

del(22)(q13.31qter) have been reported, and their clinical manifestations included MR, muscular hypotonia, midface hypoplasia with prominent mandible, high palate, prominent and dysplastic ears, sacral dimple, simple palmar crease and syndactyly, but sex reversal has never been recognized [Schinzel, 2001]. Interestingly, duplication of chromosome 22 associated with sex reversal or hermaphroditism has been reported [Aleck et al., 1999; Seeherunvong et al., 2004]. It is notable that a smallest duplication found in

an SRY-negative patient with sex reversal [Seeherunvong et al., 2004] overlapped with the 3-Mb deleted region found in this study.

46XY, del (3)(p21p21) de novo in MR126

This interstitial deletion spans a 1-Mb region from RP11-804H8 to RP11-89F17 (UCSC coordinates, chromosome 3 nucleotide 50533657–51559095). Neither of his parents had the deletion. Among

TABLE I. Clinical Manifestations of MR Patients With Submicroscopic Chromosomal Abnormalities

| Case	Karyotype	Sex	Age	Size (Mb) of imbalance	MR	Clinical manifestation besides mental retardation
MR88	46XY,del(15)(q11.2q12)mat	M	3	0.7	Severe	Angelman syndrome (epilepsy, ataxic gait, happy disposition, characteristic facial features, disrupted sleep)
MR96	46,XX,del(1)(1q43qter)	F	3	9.1	n.d.	IUGR, growth abnormalities, dysmorphic facial features, but detailed information unavailable
MR118	46XY,der(22) t(19;22)(p13.3;q13.31)pat	F	4	5.8/2.9	Severe	Sex reversal (uterus present, no detectable gonad), IUGR, severe growth and developmental delay, facial dysmorphology, patent ductus arteriosus, duodenal atresia
MR126	46XY,del (3)(p21p21)de novo	M	5	1.0	Moderate	Postnatal growth retardation, hypotonia, facial dysmorphology, left Sprengel deformity, short fingers, single palmar crease of left hand, micropenis
MR135	46XY,dup(22)(q11)de novo	M	7	2.2	Mild	Learning disability, motor delay, brachydactyly, right cryptorchidism
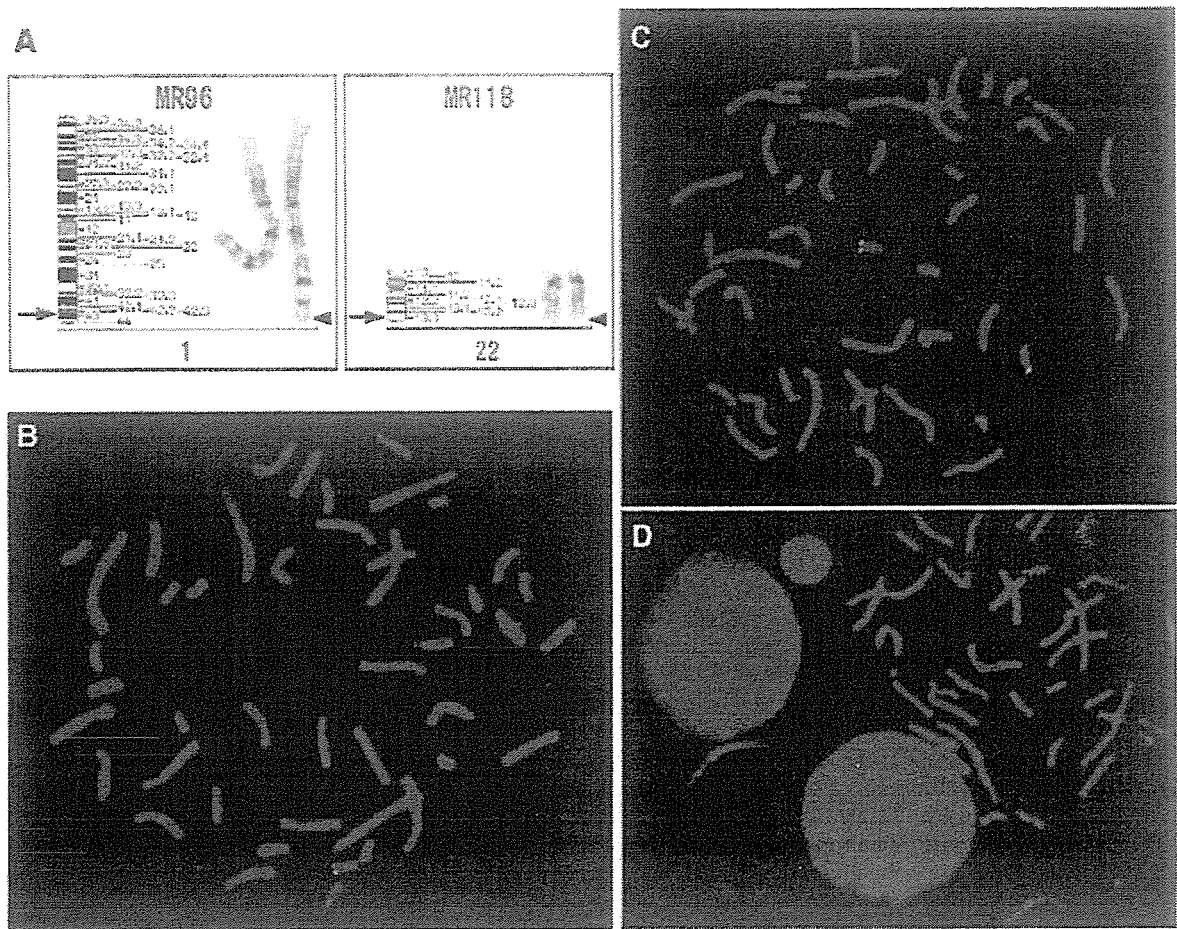
Fig. 3. Abnormal partial karyotypes of MR96 and MR118 which were later confirmed by G-banded chromosomal analysis (550 bands) (A) and FISH analysis using RP11-241K5 (SpectrumOrange, red) at 19p13.3 and RP11-125K3 (SpectrumGreen, green) at 22q13.31 on metaphase chromosomes of MR118 (B) with 46XY,der(22)t(19;22)(p13.3;q13.31)pat and father of MR118 (C) with 46XY,t(19;22)(p13.3;q13.31). In MR135 (D), FISH signals of RP11-316L10 (SpectrumOrange, red) at 22q11.2 on metaphase chromosomes and interphase nuclei. Heterozygous duplication is clearly demonstrated.

26 genes mapped to the deleted region, *DOCK3* and *GRM2* are expressed in the neuronal system.

de Silva et al. [2003] reported a pedigree with attention deficit hyperactivity disorder (ADHD) associated with inv(3)(p14:q21). These inversion breakpoints destroyed the *DOCK3* at 3p14 as well as *SLC9L9* at 3q21. The average IQ score of the family member with this inversion is significantly lower (IQ = 76.6) than without inversion (IQ = 93.7) (*P* = 0.03) [de Silva et al., 2003], indicating that *DOCK3* haploinsufficiency may be related to MR in MR126. *DOCK3* is expressed mainly in human brain and testis (but not in sperm), and in mice, *Dock3* expression was observed predominantly in adult brain.

46XY,dup(22)(q11.2q11.2)de novo in MR135

The duplication spanned a 2.2-Mb region from RP11-1151A3 to RP11-505B16 (UCSC coordinates, chromosome 22 nucleotide 17440503–19667441) similar to the previously reported duplication that complements the velocardiofacial 22q11 microdeletion (Figs. 1B and 3D) [Ensenauer et al., 2003; Hassed et al., 2004; Yobb et al., 2005]. Clinical manifestations in MR135 include mild MR including learning disability, motor delay, brachydactyly, and right cryptorchidism, most of which are compatible to those reported (Table I) [Ensenauer et al., 2003; Hassed et al., 2004; Yobb et al., 2005]. Parental chromosomes did not harbor the duplication.

Copy Number Polymorphisms

Among 43 loci showing copy number changes in patients, 9 were observed in either of parents, and 16 were also observed in another series of patients with Kabuki make-up syndrome [Miyake et al., 2005], implying that they are likely CPNs as these loci were not only observed in individuals with different phenotypes but also in normal controls. Actually nine of them were registered in the database of genomic variants (http://projects.tcag.ca/variation/). Other

nine clones remains inconclusive as parental samples were not obtained.

DISCUSSION

In order to set up a high-quality BAC aCGH system, it was critical to collect appropriate BAC clones showing a single signal on the expected chromosomal region by FISH analysis. Surprisingly, our FISH analysis indicated that almost 13% of "FISHed" clones were not suitable for aCGH as they gave another/other cross-hybridized signal(s) on an unexpected chromosome(s) (especially on the centromere region) as well as an appropriate signal (multiple signals) or an aberrant signal on a different chromosomal location probably due to contamination. Elimination of these clones is a time-consuming and arduous process, but is very important to increase reliability and minimize errors and misinterpretations. According to the study using DNAs from a normal control and a complex chromosomal abnormality, [46,XX,inv dup del(8)(qter → p23.1:: p23.1 → p11.23:)], a cut-off value was set to ±3 SD where sensitivity was 100%, specificity 99.3%, false positive rate 0.66%, and false negative rate 0%.

We detected 5 chromosome aberrations in 5 out of 30 MR patients (17%), the frequency being similar to previous data. [Vissers et al., 2003; Shaw-Smith et al., 2004]. Two of five chromosomal abnormalities involved subtelomeric regions, supporting that the subtelomere-specific microarray would be the first choice for genomic analysis of idiopathic MR in terms of cost-effectiveness. The detection-rate of interstitial microdeletion/duplication in our MR series is 10% (3/30), comparative to that of subtelomeric changes (7%, 2/30) in our series.

Recent studies indicate CPNs are fairy common even in normal human genomes [Iafrate et al., 2004; Sebat et al., 2004; Buckley et al., 2005]. Assuming that CPNs found in this study and the database are hundreds kb or more in size, their potential effects on human phenotypes could be more significant than those of single nucleotide polymorphisms. Accumulation of CPN data is obviously important to differentiate pathological changes in relation to human diseases from mere CPNs without any significant phenotypic effects.

In conclusion, our BAC aCGH with a resolution of 1.5 Mb for the whole genome successfully identified five disease-causing submicroscopic chromosomal aberrations as well as 22 or more CPNs in MR patients. Higher resolution array such as whole genome tiling array could provide a detailed list of MR-related genes as well as CPNs.

ACKNOWLEDGMENTS

REFERENCES

Aleck KA, Argueso L, Stone J, Hackel JG, Erickson RP. 1999. True hermaphroditism with partial duplication of chromosome 22 and without SRY. Am J Med Genet 85:2–4.

Buckley PG, Mantripragada KK, Piotrowski A, Diaz de Stahl T, Dumanski JP. 2005. Copy-number polymorphisms: Mining the tip of an iceberg. Trends Genet 21:315–317.

de Silva MG, Elliott K, Dahl HH, Fitzpatrick E, Wilcox S, Delatycki M, Williamson R, Efron D, Lynch M, Forrest S. 2003. Disruption of a novel member of a sodium/hydrogen exchanger family and DOCK3 is associated with an attention deficit hyperactivity disorder-like phenotype. J Med Genet 40:733–740.

de Vries BB, White SM, Knight SJ, Regan R, Homfray T, Young ID, Super M, McKeown C, Splitt M, Quarrell OW, Trainer AH, Niermeijer MF, Malcolm S, Flint J, Hurst JA, Winter RM. 2001. Clinical studies on submicroscopic subtelomeric rearrangements: A checklist. J Med Genet 38:145–150.

de Vries BB, Winter R, Schinzel A, van Ravenswaaij-Arts C. 2003. Telomeres: A diagnosis at the end of the chromosomes. J Med Genet 40:385–398.

Ensenauer RE, Adeyinka A, Flynn HC, Michels VV, Lindor NM, Dawson DB, Thorland EC, Lorentz CP, Goldstein JL, McDonald MT, Smith WE, Simon-Fayard E, Alexander AA, Kulharya AS, Ketterling RP, Clark RD, Jalal SM. 2003. Microduplication 22q11.2, an emerging syndrome: Clinical, cytogenetic, and molecular analysis of thirteen patients. Am J Hum Genet 73:1027–1040.

Fiegler H, Carr P, Douglas EJ, Burford DC, Hunt S, Scott CE, Smith J, Vetrie D, Gorman P, Tomlinson IP, Carter NP. 2003. DNA microarrays for comparative genomic hybridization based on DOP-PCR amplification of BAC and PAC clones. Genes Chromosomes Cancer 36:361–374.

Flint J, Wilkie AO, Buckle VJ, Winter RM, Holland AJ, McDermid HE. 1995. The detection of subtelomeric chromosomal rearrangements in idiopathic mental retardation. Nat Genet 9:132–140.

Harada N, Hatchwell E, Okamoto N, Tsukahara M, Kurosawa K, Kawame H, Kondoh T, Ohashi H, Tsukino R, Kondoh Y, Shimokawa O, Ida T, Nagai T, Fukushima Y, Yoshiura K, Niikawa N, Matsumoto N. 2004. Subtelomere specific microarray based comparative genomic hybridisation: A rapid detection system for cryptic rearrangements in idiopathic mental retardation. J Med Genet 41:130–136.

Hassed SJ, Hopcus-Niccum D, Zhang L, Li S, Mulvihill JJ. 2004. A new genomic duplication syndrome complementary to the velocardiofacial (22q11 deletion) syndrome. Clin Genet 65:400–404.

Iafrate AJ, Feuk L, Rivera MN, Listewnik ML, Donahoe PK, Qi Y, Scherer SW, Lee C. 2004. Detection of large-scale variation in the human genome. Nat Genet 36:949–951.

Knight SJ, Regan R, Nicod A, Horsley SW, Kearney L, Homfray T, Winter RM, Bolton P, Flint J. 1999. Subtle chromosomal rearrangements in children with unexplained mental retardation. Lancet 354:1676–1681.

Kurosawa K, Harada N, Sosonkina N, Niikawa N, Matsumoto N, Saitoh S. 2004. Unmasking 15q12 deletion using microarray-based comparative genomic hybridization in a mentally retarded boy with r(Y). Am J Med Genet Part A 130A:322–324.

Miyake N, Tonoki N, Gallegp M, Harada N, Shimokawa O, Yoshiura K, Ohta T, Kishino T, Niikawa N, Matsumoto N. 2004.

Phenotype–genotype correlation in two patients 12q proximal deletion. J Hum Genet 49:282–284.

Miyake N, Shimokawa O, Harada N, Sosonkina N, Okubo A, Kawara H, Okamoto N, Ohashi H, Kurosawa K, Naritomi K, Kaname T, Nagai T, Shotelersuk V, Hou J-H, Fukushima Y, Kondoh T, Matsumoto T, Shinoki T, Kato M, Tonoki T, Nomura M, Yoshiura K-i, Kishino T, Ohta T, Niikawa N, Matsumoto N. 2005. No causative genomic aberrations by BAC array CGH in Kabuki make-up syndrome. Am J Med Genet (in this issue).

Schinzel A. 2001. Catalogue of unbalanced chromosome aberrations in man. 2nd edition. New York: Walter de Gruyter.

Sebat J, Lakshmi B, Troge J, Alexander J, Young J, Lundin P, Maner S, Massa H, Walker M, Chi M, Navin N, Lucito R, Healy J, Hicks J, Ye K, Reiner A, Gilliam TC, Trask B, Patterson N, Zetterberg A, Wigler M. 2004. Large-scale copy number polymorphism in the human genome. Science 305:525–528.

Seeherunvong T, Perera EM, Bao Y, Benke PJ, Benigno A, Donahue RP, Berkovitz GD. 2004. 46,XX sex reversal with partial duplication of chromosome arm 22q. Am J Med Genet Part A 127A:149–151.

Shaw-Smith C, Redon R, Rickman L, Rio M, Willatt L, Fiegler H, Firth H, Sanlaville D, Winter R, Colleaux L, Bobrow M, Carter NP. 2004. Microarray based comparative genomic hybridisation (array-CGH) detects submicroscopic chromosomal deletions and duplications in patients with learning disability/mental retardation and dysmorphic features. J Med Genet 41:241–248.

Vissers LE, de Vries BB, Osoegawa K, Janssen IM, Feuth T, Choy CO, Straatman H, van der Vliet W, Huys EH, van Rijk A, Smeets D, van Ravenswaaij-Arts CM, Knoers NV, van der Burgt I, de Jong PJ, Brunner HG, van Kessel AG, Schoenmakers EF, Veltman JA. 2003. Array-based comparative genomic hybridization for the genomewide detection of submicroscopic chromosomal abnormalities. Am J Hum Genet 73:1261–1270.

Yobb TM, Somerville MJ, Willatt L, Firth HV, Harrison K, Mackenzie J, Gallo N, Morrow BE, Shaffer LG, Babcock M, Chernos J, Bernier F, Sprysak K, Christiansen J, Haase S, Elyas B, Lilley M, Bamforth S, McDermid HE. 2005. Microduplication and triplication of 22q11.2: A highly variable syndrome. Am J Hum Genet 76:865–876.

Clinical Report

Narrowing Candidate Region for Monosomy 9p Syndrome to a 4.7-Mb Segment at 9p22.2-p23

Hiroki Kawara,[1] Toshiyuki Yamamoto,[2] Naoki Harada,[1,3] Koh-ichiro Yoshiura,[3,4]
Norio Niikawa,[3,4] Akira Nishimura,[3,5] Takeshi Mizuguchi,[3,5] and Naomichi Matsumoto[3,5]*

[1]Kyusyu Medical Science Nagasaki Laboratory, Nagasaki, Japan
[2]Division of Medical Genetics, Kanagawa Children's Medical Center, Yokohama, Japan
[3]CREST, Japan Science and Technology Agency, Kawaguchi, Japan
[4]Department of Human Genetics, Nagasaki University Graduate School of Biomedical Sciences, Nagasaki, Japan
[5]Department of Human Genetics, Yokohama City Graduate School of Medicine, Yokohama, Japan

A 2-year-old boy with clinical manifestations of monosomy 9p syndrome and brown hair is described. G-banding and chromosome FISH studies demonstrated complex rearrangements involving seven breakpoints in chromosomes 2 and 9, which included a 6.6-Mb deletion at 9p22.2-p23. This, together with previous studies in the literature, narrowed the shortest region of overlap (SRO) for the syndrome to a 4.7-Mb interval. Candidate genes for trigonocephaly, mental retardation, and brown hair are discussed.
© 2006 Wiley-Liss, Inc.

Key words: monosomy 9p syndrome; shortest region of overlap; trigonocephaly; mental retardation; brown hair

INTRODUCTION

Trigonocephaly is a type of craniosynostosis characterized by a triangular shape of the skull, caused by premature closure of the metopic suture, with its prevalence estimated at one in 10,000–15,000 births [Lajeunie et al., 1998]. It is seen in a number of genetic disorders and chromosome abnormalities with several different genetic conditions including autosomal dominant, autosomal recessive, and X-linked recessive forms; monosomy 9p syndrome, partial 11q monosomy syndrome (also known as Jacobsen syndrome), and Opitz C syndrome. Monosomy 9p syndrome is caused by a deletion spanning 9p22-p24. Its clinical manifestations include mental retardation, trigonocephaly, midface hypoplasia, upward-running palpebral fissures, and long philtrum [Christ et al., 1999]. Its critical region is at an 8-Mb interval between *D9S286* and *D9S285* [Christ et al., 1999; Jehee et al., 2005].

We here describe a boy with clinical manifestations of monosomy 9p syndrome and complex rearrangements involving chromosomes 2 and 9. Evidence will be presented that the candidate region for the syndrome is in a 4.7-Mb interval at 9p22.2-p23.

CLINICAL REPORT

The proband, a boy, was born at 41 weeks of gestation as the first child of a 35-year-old, G1P1 mother and a 31-year-old non-consanguineous father. Birth weight was 3,256 g (+0.1 SD), length 48.9 cm (+0.4 SD), and OFC 34.5 cm (+0.7 SD). Transient heart murmurs were audible. When referred to us at age 12 months for developmental delay, he weighed 7,720 kg (−1.78 SD), measured 75 cm (mean), and had OFC of 43.4 cm (−2 SD). He could neither sit alone or turn over. Abnormalities noted included trigonocephaly, microcephaly, brown hair; characteristic face with upslanting palpebral fissures, telecanthus, flat nasal bridge, small and malformed ears, anteverted nostrils, long philtrum; and mild hypospadias (Fig. 1A). Skin color was relatively light. His DQ was estimated to be 38. Brain MRI showed agenesis of the corpus callosum. Hearing was not impaired. The metopic suture was
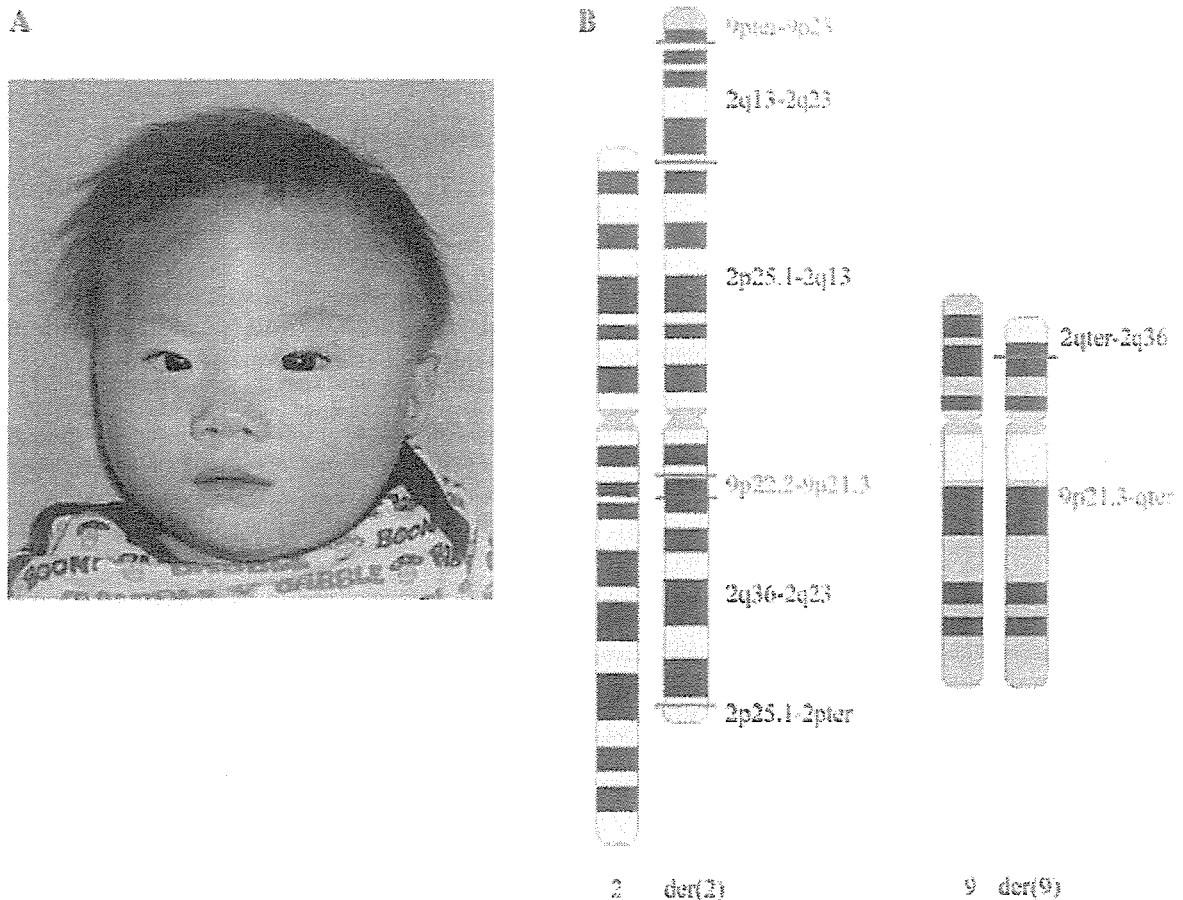
A   B

Fig. 1. A: The patient at age 12 months. B: Partial karyotype of chromosomes 2 and 9.

surgically separated at age 14 months. He sat alone at 18 months. At age 2 years, his development was moderately delayed: he neither walked nor spoke any word.

CYTOGENETIC ANALYSIS

G-banding analysis of cultured peripheral blood lymphocytes from the patient indicated a three-way translocation involving the 2p24-pter, 2q36-qter and 9p22-pter segments; and an intrachromosomal shift of a 2q13-q23 segment to a position next to band 2p25.1, as well as an inverted 2q23-2q36 segment attached next to band 2q13. The chromosomes of his parents were normal. Spectral karyotyping of the patient's chromosomes (performed by SRL, Hachioji, Japan) indicated involvement of the 2p and 9p regions, but was otherwise non-contributory (data not shown). FISH analysis of the 9p and 2p25.1 regions, using a series of RPCI-11 BAC clones as probes, disclosed an insertion of a 9p21.3-p22.2 segment into band 2q13 and a 9p22.2-p23 deletion, both undetectable by G-band analysis (Figs. 1B

and 2A). Further FISH studies refined the breakpoints of these rearrangements (Figs. 2 and 3). The 9p22.2-p23 deletion spanned a 6.6-Mb segment ranging from RP11-933C16 to RP11-711J1 (UCSC coordinate, chromosome 9 nucleotides 11355596-17941657). The rearrangements thus involved seven break-points (2p25.1, 2q13, 2q23, 2q36, 9p23, 9p22.2, and 9p21.3) and included a submicroscopic dele-tion at 9p21.3-p23. The patient's karyotype accord-ing to ISCN 2005 was thus interpreted as 46,XY, der(2)(9pter → 9p23::2q13 → 2q23::2p25.1→ 2q13:: 9p22.2 → 9p21.3::2q36 →2q23::2p25.1 → 2pter), der(9)(2qter → 2q36::9p21.3 → 9qter)de novo.

DISCUSSION

The 2-year-old boy we have described had clinical manifestations typical of the monosomy 9p syn-drome, including mental retardation (present in 100% of patients with this syndrome), trigonocephaly (84%), upward running palpebral fissures (66%), epicanthal folds (74%), flat nasal bridge (85%),

A 9p22.2-p23 REGION
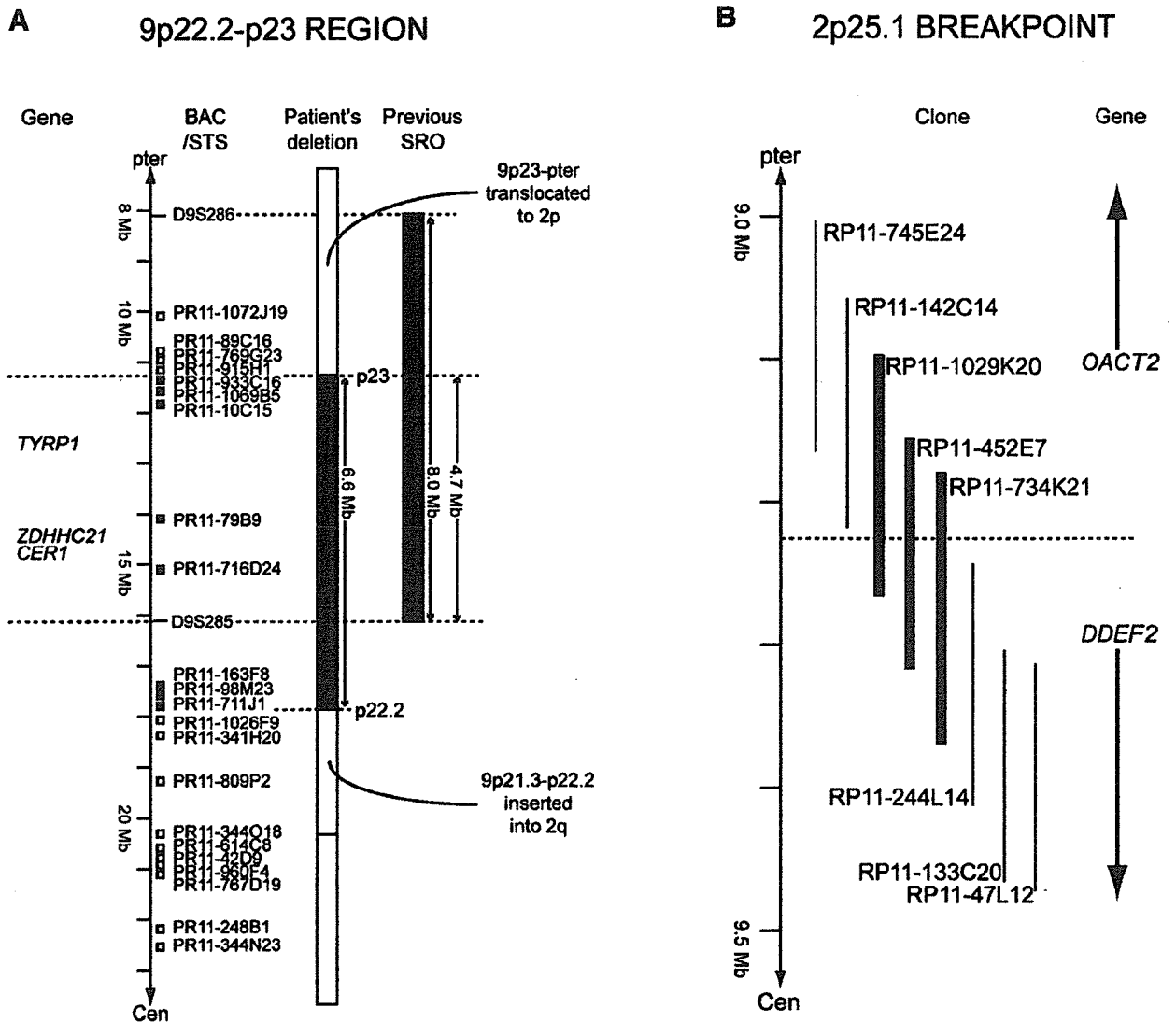
B 2p25.1 BREAKPOINT

Fig. 2. **A:** Physical map spanning the 9p22.2-p23 deletion region. Open-squares indicate non-deleted clones, closed squares denote deleted clones. **B:** Physical map of the 2p25.1 breakpoint region. Thick lines indicate the clones that span the breakpoint. Genes *OACT2* and *DDEF2* are situated close to, but not involved in, the breakpoint.

anteverted nostrils (84%), long philtrum (90%), small and malformed ears (84%), hypospadias (cryptorchidism or malformed genitalia, 45%), and heart murmurs (cardiopathy or hear murmurs, 48%) [Huret et al., 1988; Jehee et al., 2005]. The boy had a 6.6-Mb deletion at 9p22.2-p23. Previous studies on patients with the monosomy 9p syndrome have defined a shortest region of overlap (SRO) at an 8.0-Mb segment, spanning *D9S286* and *DS285* loci (UCSC coordinate, chromosome 9 nucleotides 8043378-16068221) [Christ et al., 1999; Jehee et al., 2005]. Adding the data from the boy we described, the SRO may be narrowed to a 4.7-Mb segment from RP11-933C16 to D9S285 (Fig. 2A).

The 4.7-Mb interval contains at least 10 known genes. Among them, a deletion of *CER1* may cause

trigonocephaly (Fig. 2A). *CER1*, encoding a Cerrerus-related protein, may play a role in the anterior neural induction and somite formation during embryogenesis, in part through a BMP-inhibitory mechanism [Biben et al., 1998; Shawlot et al., 1998]. Deletion of *ZDHHC21* (the zinc finger, DHHC domain containing 21 gene) may contribute to mental retardation. Loss of expression of *ZDHHC15*, a homolog of *ZDHHC21*, was shown to result in severe mental retardation in a woman with a balanced t(X;15) translocation [Mansouri et al., 2005]. Deletion of *TYRP1* (the tyrosinase-related protein 1 gene) may have caused the brown hair in the boy we have described. Homozygous or compound heterozygous mutations of *TYRP1* may result in Rufous oculocutaneous albinism and oculocutaneous albinism
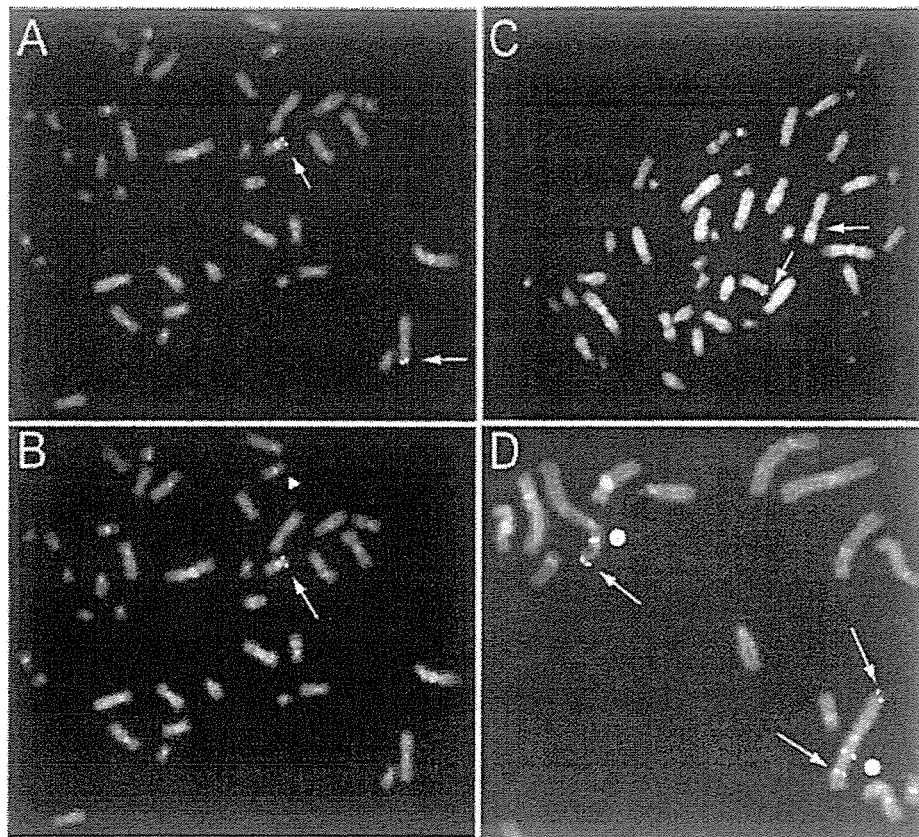
Fig. 3. **A–C:** FISH analysis of the 9p22-p23 deletion segment region using clones, RP11-915H1 (A), RP11-933C16 (B), and RP11-1026F9 (C). Arrow indicates a positive signal, and arrowhead an absent signal. Signals for RP11-915H1 and RP11-1026F9 are translocated to der(2), while those for RP11-933C16 are missing from der(9). **D:** FISH analysis of the 2p25.1 breakpoint region of der(2). Arrows show signals of RP11-734K21 and globule for RP11-634M21 serving as a marker at 2p16. Split signals for RP11-734K21 were seen on der(2).

type 3 [Boissy et al., 1996; Manga et al., 1997]. Analogy may be drawn from the light skin color in the patient with Prader–Willi and Angelman syndromes with 15q11-q13 deletion including the *P* gene, whose homozygous or compound heterozygous mutations cause autosomal recessive oculocutaneous albinism type 2 [Lossie et al., 2001].

Opitz "C" trigonocephaly-like syndrome has been described in patients with terminal deletion 2p and partial duplication of 17q [Czako et al., 2004]. In view of the presence of 2p25.1 breakpoint in the der(2) chromosome in the boy we described, the possibilities was explored of disruption or dysfunction of a gene spanning or situated close to the breakpoint, which in turn may cause trigonocephaly (Fig. 2B). Two genes, *DDEF2* and *OACT2* are mapped close to the breakpoint, but there is no obvious link of their function to trigonocephaly.

ACKNOWLEDGMENTS

We are grateful to the family for their participation in this study and consent to publication of the boy's

REFERENCES

Biben C, Stanley E, Fabri L, Kotecha S, Rhinn M, Drinkwater C, Lah M, Wang CC, Nash A, Hilton D, Ang SL, Mohun T, Harvey RP. 1998. Murine cerberus homologue mCer-1: A candidate anterior patterning molecule. Dev Biol 194:135–151.

Boissy RE, Zhao H, Oetting WS, Austin LM, Wildenberg SC, Boissy /SNM> YL, Zhao Y, Sturm RA, Hearing VJ, King RA, Nordlund JJ. 1996. Mutation in and lack of expression of tyrosinase-related protein-1 (TRP-1) in melanocytes from an individual with brown oculocutaneous albinism: A new subtype of albinism classified as "OCA3". Am J Hum Genet 58:1145–1156.

Christ LA, Crowe CA, Micale MA, Conroy JM, Schwartz S. 1999. Chromosome breakage hotspots and delineation of the critical region for the 9p-deletion syndrome. Am J Hum Genet 65:1387–1395.

Czako M, Riegel M, Morava E, Bajnoczky K, Kosztolanyi G. 2004. Opitz "C" trigonocephaly-like syndrome in a patient with terminal deletion of 2p and partial duplication of 17q. Am J Med Genet Part A 131A:310–312.

Huret JL, Leonard C, Forestier B, Rethore MO, Lejeune J. 1988. Eleven new cases of del(9p) and features from 80 cases. J Med Genet 25:741–749.

Jehee FS, Johnson D, Alonso LG, Cavalcanti DP, de Sa Moreira E, Alberto FL, Kok F, Kim C, Wall SA, Jabs EW, Boyadjiev SA, Wilkie AO, Passos-Bueno MR. 2005. Molecular screening for microdeletions at 9p22-p24 and 11q23-q24 in a large cohort of patients with trigonocephaly. Clin Genet 67:503–510.

Lajeunie E, Le Merrer M, Marchac D, Renier D. 1998. Syndromal and nonsyndromal primary trigonocephaly: Analysis of a series of 237 patients. Am J Med Genet 75:211–215.

Lossie AC, Whitney MM, Amidon D, Dong HJ, Chen P, Theriaque D, Hutson A, Nicholls RD, Zori RT, Williams CA, Driscoll DJ. 2001. Distinct phenotypes distinguish the molecular classes of Angelman syndrome. J Med Genet 38:834–845.

Manga P, Kromberg JG, Box NF, Sturm RA, Jenkins T, Ramsay M. 1997. Rufous oculocutaneous albinism in southern African Blacks is caused by mutations in the TYRP1 gene. Am J Hum Genet 61:1095–1101.

Mansouri MR, Marklund L, Gustavsson P, Davey E, Carlsson B, Larsson C, White I, Gustavson KH, Dahl N. 2005. Loss of ZDHHC15 expression in a woman with a balanced translocation t(X;15)(q13.3;cen) and severe mental retardation. Eur J Hum Genet.

Shawlot W, Deng JM, Behringer RR. 1998. Expression of the mouse cerberus-related gene, Cerr1, suggests a role in anterior neural induction and somitogenesis. Proc Natl Acad Sci USA 95:6198–6203.

ORIGINAL ARTICLE

Remco Visser · Tomonobu Hasegawa · Norio Niikawa
Naomichi Matsumoto

Analysis of the *NSD1* promoter region in patients with a Sotos syndrome phenotype

Abstract Sotos syndrome (SoS, OMIM#117550) is an overgrowth disorder characterized by excessive growth—especially in the first years of childhood—distinctive craniofacial features, and various degrees of mental retardation. Haploinsufficiency of the nuclear receptor binding SET domain containing protein 1 (*NSD1*) gene, due to either intragenic mutations or whole-gene microdeletions, is found in the majority of patients with SoS. However, in approximately 10–40% of patients with a typical SoS phenotype, no abnormalities are detected. In this study, hemizygous hypermethylation or genomic sequence abnormalities of the promoter region of *NSD1* were hypothesized to be the underlying cause in patients with a SoS phenotype, but without confirmed *NSD1* alterations. In 18 patients, including one patient with a reported hepatocellular carcinoma, the promoter region of *NSD1* was analyzed. However, no hypermethylation or sequence abnormalities in the promoter region could be detected. It therefore seems unlikely that such abnormalities of *NSD1* are a major culprit in patients with phenotypical SoS. Additional methods are necessary for detection of other genetic or epigenetic causes of SoS.

Keywords Epimutation · Methylation · *NSD1* · Promoter · Sotos syndrome

Abbreviations BWS: Beckwith–Wiedemann syndrome · *NSD1*: Nuclear receptor binding SET domain containing protein 1 · *NSD2*: Nuclear receptor binding SET domain containing protein 2 · *NSD3*: Nuclear receptor binding SET domain containing protein 3 · SNP: Single nucleotide polymorphism · SoS: Sotos syndrome

R. Visser · N. Niikawa
Department of Human Genetics, Nagasaki University Graduate
School of Biomedical Sciences, Nagasaki, Japan

R. Visser
Department of Pediatrics,
Leiden University Medical Center, Leiden, The Netherlands

R. Visser · N. Matsumoto (✉)
Department of Human Genetics, Yokohama City University
Graduate School of Medicine, 3-9 Fukuura, Kanazawa-ku,
Yokohama 236-0004, Japan
E-mail: naomat@yokohama-cu.ac.jp
Tel.: +81-45-7872606
Fax: +81-45-7865219

R. Visser · N. Niikawa · N. Matsumoto
CREST, Japan Science and Technology Agency,
Kawaguchi, Japan

R. Visser · N. Niikawa
International Consortium for Medical Care of Hibakusha and
Radiation Life Science, The 21st Century Center of Excellence,
Nagasaki, Japan

T. Hasegawa
Department of Pediatrics, Keio University School of Medicine,
Tokyo, Japan

Introduction

Sotos syndrome (SoS, OMIM#117550) is a congenital overgrowth syndrome with characteristic craniofacial features and variable degrees of developmental delay (Cole and Hughes 1994). Aberrations of the nuclear receptor binding SET domain containing protein 1 (*NSD1*) gene at 5q35 include intragenic mutations and submicroscopic whole-gene deletions (Kurotaki et al. 2002, 2003; Douglas et al. 2003; Nagai et al. 2003; Rio et al. 2003; Turkmen et al. 2003; de Boer et al. 2004; Tatton-Brown et al. 2005). In approximately 10–40% of typical SoS patients without a detected *NSD1* abnormality, different aberrations of *NSD1* or locus heterogeneity should be considered [see review by Visser and Matsumoto (2003)]. In two SoS patients, abnormalities were detected in the imprinted region of 11p15, which is a common cause of Beckwith–Wiedemann syndrome (BWS, OMIM#130850) (Baujat et al. 2004). However, to date, no new cases are reported. Furthermore, a

screening of the *NSD*-gene family in patients with a SoS phenotype, but without *NSD1* aberrations, excluded involvement of *NSD2* and *NSD3* (Douglas et al. 2005).

In cancer genetics, epigenetic changes in tumors, such as promoter methylation of tumor repressor genes, are well known to result in transcriptional silencing of genes (Baylin and Herman 2000). Recently, in two individuals with multiple colorectal tumors, germline hypermethylation of the DNA mismatch repair gene *MLH1* was identified (Suter et al. 2004). Similar epimutations of the promoter region of *NSD1* were hypothesized to be responsible for transcriptional silencing of *NSD1* and would subsequently lead to SoS. In this study, 18 patients with a typical SoS phenotype but without aberrations of *NSD1* were screened for epimutations. Furthermore, the promoter regions were sequenced in all patients to exclude possible genomic mutations.

Materials and methods

Patients

The study population comprised of 18 patients with characteristic SoS features, in whom *NSD1* abnormalities were excluded. Seventeen patients were reported previously (Kurotaki et al. 2002, 2003; Kamimura et al. 2003) and one was newly added. The clinical inclusion criteria and the methods for *NSD1* analysis, consisting of gene sequencing and FISH analysis, have been reported elsewhere (Kamimura et al. 2003; Kurotaki et al. 2003). After informed consent, genomic DNA was obtained from peripheral blood cells. Experimental protocols were approved by the Committee for Ethical Issues at Yokohama City University School of Medicine, and by the Committee for Ethical Issues on Human Genome and Gene Analysis at Nagasaki University.

NSD1 promoter region

A 7.2-kb sequence was downloaded from the National Center for Biotechnology Information (NCBI) build 35 database (May 2004) available on the UCSC Genome Bioinformatics web site (http://genome.ucsc.edu/). This sequence includes the starting sites of the two known transcripts of *NSD1*: the shorter variant 1 (GenBank accession number NM_172349) and the longer variant 2 (GenBank accession number NM_022455). Furthermore, it extends 5 kb upstream from the most proximal transcript (variant 2). The following programs were used for predictions of promoter locations and CpG-islands: CpG-promoter (http://rulai.cshl.org/tools/CpG_promoter/) (Ioshikhes and Zhang 2000), FirstEF (http://rulai.cshl.org/tools/FirstEF/) (Davuluri et al. 2001), and CpGProD (http://pbil.univ-lyon1.fr/software/cpgprod_query.html) (Ponger and Mouchiroud 2002). If masking of repeats was deemed necessary (Bajic et al. 2004), the RepeatMasker webserver was used (http://

www.repeatmasker.org/). Only promoter predictions coinciding with a correct prediction of the first exon (according to transcript variants 1 and 2) were kept in analysis. Transcription factor-binding sites were identified using the DNASIS Pro software (Hitachi Software Engineering Co., Tokyo, Japan).

Evaluation of the methylation status of the *NSD1* promoter region

The DNA was treated with sodium bisulfite according to the manufacturer's guidelines (CpGenome™ DNA Modification Kit, Chemicon International, Temecula, CA, USA). Polymerase chain reaction (PCR) was performed in a 25 µl mixture containing 0.8 µM of each primer, 1 unit of JumpStart™ REDTaq™ DNA polymerase (Sigma, St. Louis, MO, USA), 0.2 mM of each dNTP and 1× PCR buffer. Conditions included initial denaturation at 94°C for 2 min, 45 cycles of 94°C for 30 s, 60°C for 30 s, 72°C for 40 s, and a final extension of 72°C for 7 min. Primers for bisulfite PCR (degenerate and non-degenerate primers) were designed with Methprimer (http://www.urogene.org/methprimer/index1.html) (Li and Dahiya 2002) and Primer3 (http://frodo.wi.mit.edu/cgi-bin/primer3/primer3_www.cgi) (Rozen and Skaletsky 2000). Degenerate primers were designed if primers contained a CpG nucleotide. Primers are *forward* 5′-GAGTTGTTGTTTTTATTTTGTTTTTTGT-3′ and *reverse* 5′-CCCTTCTCTCACTCTTC*R*AAATTC-3′. This PCR product was subsequently subjected to nested PCR with the following primers: *forward* 5′-GGTGGTGGTGTGGGTTTG-3′ and *reverse* 5′-CTCTCACTCTTC*R*AAATTCAAAAC-3′. The product was cloned with the Topo-TA kit (Invitrogen, Carlsbad, CA, USA). DNA was obtained after overnight cultures, and sequencing was performed as described previously (Visser et al. 2005).

Genomic analysis of the *NSD1* promoter region

Primers were designed with the online version of Primer3 (Rozen and Skaletsky 2000). A ~2.3 kb product was amplified with primers *forward* 5′-TGCCTCCATTTTGTTTCCTG-3′ and *reverse* 5′-CATGGAGGCCAAATCCTGTA-3′ using LaTaq (Takara Bio, Otsu, Shiga, Japan) with the provided 2× GC buffer. Nested primers were used for sequencing. All primers and conditions are available upon request.

Results

The identified CpG-islands by CpGProD and CpG-promoter and the prediction of promoter locations by FirstEF are shown in Fig. 1. The region for methylation analysis was selected based on overlapping predictions and on proximity to the starting site of transcript variant
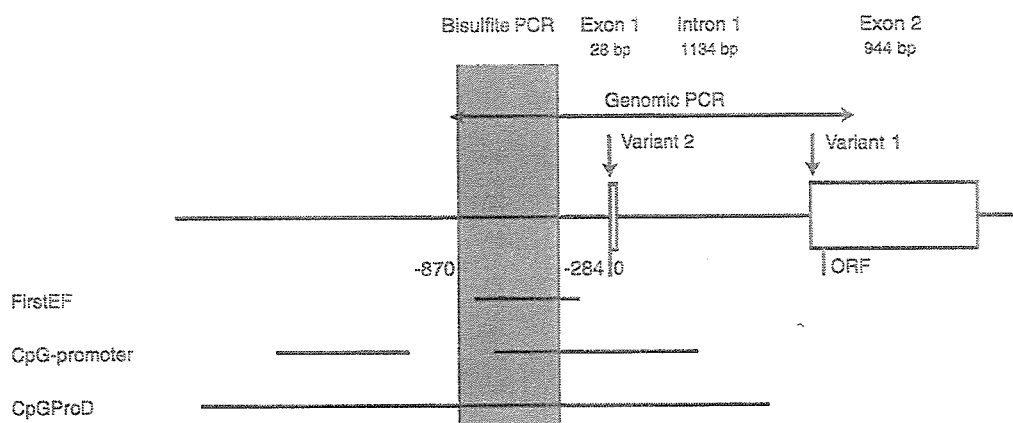
Fig. 1 Computational analysis of the promoter region of *NSD1*. *NSD1* and its 5' region (5 kb) are shown schematically. The starting sites of transcript variant 1 and variant 2 are depicted by *vertical arrows*. The first nucleotide of variant 2 (position) is used as a starting point for numbering of the nucleotides. The names of the promoter and CpG-islands prediction programs are shown on the left and their predicted promoter regions and CpG-islands are shown under the 5'-region of *NSD1*. The region amplified after bisulfite conversion is the *gray-shaded* area between the vertical lines. A *horizontal bidirectional arrow* depicts ~2.3 kb PCR product used for genomic sequencing. *bp* base-pair, *ORF* open reading frame

2. Bisulfite PCR and subsequent nested PCR produced a product of 587 bp containing a total of 60 CpGs. Sequence information was obtained with a single reverse primer for a total of 46 most proximally located CpGs. For each patient, at least 18 clones were analyzed to ensure an accurate distribution of possible methylated and non-methylated clones. A total number of 18 SoS patients were analyzed, including one patient with a confirmed well-differentiated hepatocellular carcinoma. In all patients with SoS, no hypermethylation of the analyzed region was detected (Fig. 2). In some patients (SoS 58, SoS 62, and SoS 113), single hypermethylated cytosine-nucleotides were found. In SoS 113, a putative AP-2 transcription factor-binding site was identified to be co-localizing with such a hypermethylated CpG nucleotide (Fig. 2).

A ~2.3 kb product was amplified containing the genomic region of ~0.9 kb proximal of exon 1 until within exon 2 (Fig. 1). None of the 18 patients showed any mutations within this region. In the NCBI SNP database build 124 (http://www.ncbi.nlm.nih.gov/SNP/), only a C/T polymorphism was deposited for this region (refSNP ID, rs3733873). Ten patients were homozygous C/C, five homozygous T/T, and three patients were heterozygous for this SNP.

Discussion

Mutations and deletions of *NSD1* account for the majority of patients with SoS (Kurotaki et al. 2002, 2003; Douglas et al. 2003; Nagai et al. 2003; Rio et al. 2003; Turkmen et al. 2003; de Boer et al. 2004; Tatton-Brown et al. 2005). However, in a considerable group of patients with characteristic SoS features, no abnormalities of *NSD1* can be detected. In this study, we hypothesized that heterozygous hypermethylation or sequence abnormalities of the promoter region of *NSD1* would lead to impairment of the gene expression. However, the 18 patients analyzed did not show methylation changes of this region, nor did sequence analysis of the promoter region reveal any mutations. In SoS 113, a hypermethylated CpG nucleotide was found to co-localize with a putative AP-2 transcription factor-binding site. Site-specific methylation of the AP-2 transcription factor-binding site was detected in tumors in neurofibromatosis type 1, but was also found in 4/20 controls (Harder et al. 2004). However, repeated analysis of a different DNA sample of SoS 113 could not confirm this hypermethylation, favoring possible bias due to incomplete conversion during the bisulfite reaction (data not shown). Although we cannot completely exclude the influence of site-specific methylation in the repression of *NSD1*, it seems unlikely that this plays a major role in SoS patients. Intragenic microdeletions, altered splicing due to mutations in introns, aberrations affecting the yet unknown expression regulatory mechanisms of *NSD1*, or abnormalities in one of the components in the *NSD1*-related signaling pathway could be responsible for the SoS patients without confirmed *NSD1* haploinsufficiency.

In this study, *in silico* analysis was used for promoter prediction. It is known, however, that the individual programs do not always achieve a good correlation of the sensitivity and positive predictive value (Bajic et al. 2004). Although we used different programs in combination with knowledge of the starting sites of transcription, it would therefore be possible that the actual promoter region is located outside the analyzed regions and/or not related to a CpG-island. Enhancement of the computational programs is necessary for the correct promoter location.

The frequency of neoplasia in SoS is estimated to be ~2–3.9% (Cohen 1999; Rahman 2005); however, a direct involvement of *NSD1* in tumor growth in SoS is
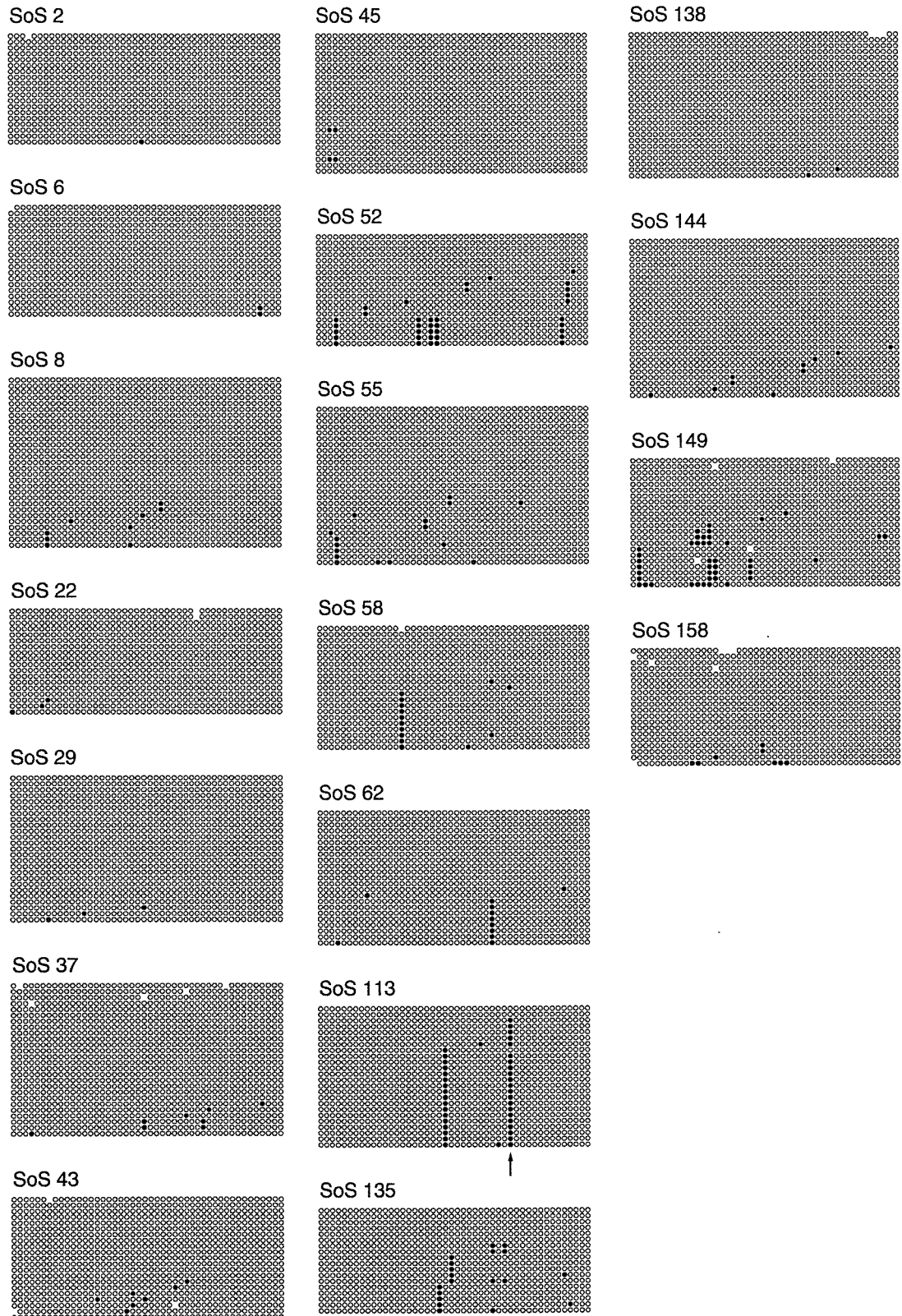
18

Fig. 2 Methylation status of CpGs per individual SoS patient. Each CpG is depicted by a *circle*. The CpGs (a total of 46) per single clone are shown horizontally and the clones are ordered vertically. *Open* and *closed circles* indicate non-methylated and methylated CpGs, respectively. *Missing circles* indicate nucleotides were the sequence could not be analyzed. A *vertical arrow* in SoS 113 indicates the position of the CpG nucleotide which co-localizes with a AP-2 transcription factor-binding site

not confirmed (Visser and Matsumoto 2003; Rahman 2005). Since the identification of *NSD1*, to our knowledge only a few SoS patients with neoplasia have been confirmed to harbor a *NSD1* alteration. This included three neuroblastomas (Nagai et al. 2003; Turkmen et al. 2003; Tatton-Brown and Rahman 2004), a ganglioglioma (Deardorff et al. 2004), a presacral ganglioneuroma, three sacrococcygeal teratomas, a small cell lung carcinoma, T-cell lymphoma, and acute lymphocytic leukaemia (Tatton-Brown and Rahman 2004; Rahman 2005). Our analysis of the methylation status of the *NSD1* promoter region could easily be applied to tumor tissues in Sotos patients with a *NSD1* alteration. Subsequently, differentiation would be possible between a primary NSD1 aberration (loss or mutation) or a combination with secondary hypermethylation, considering the Jones's newly-revised Knudson two-hit hypothesis (Knudson 1971; Jones and Laird 1999). Our patient with a hepatocellular carcinoma exhibited a specific SoS phenotype, but no alterations of *NSD1* coding regions were identified. Unfortunately, tumor tissue was not available for analysis. Further investigations in other SoS patients, with and without *NSD1* alterations, who developed neoplasia are necessary for elucidation of the possible relation between *NSD1* abnormality and neoplasia development.

In conclusion, it is unlikely that epimutations or genetic abnormalities of the *NSD1* promoter region are the main culprit for phenotypical SoS patients without yet-detected *NSD1* alterations. Future research might shed light on other genetic or epigenetic causes leading to SoS.

References

Bajic VB, Tan SL, Suzuki Y, Sugano S (2004) Promoter prediction analysis on the whole human genome. Nat Biotechnol 22:1467–1473

Baujat G, Rio M, Rossignol S, Sanlaville D, Lyonnet S, Le Merrer M, Munnich A, Gicquel C, Cormier-Daire V, Colleaux L (2004) Paradoxical NSD1 mutations in Beckwith–Wiedemann syndrome and 11p15 anomalies in Sotos syndrome. Am J Hum Genet 74:715–720

Baylin SB, Herman JG (2000) DNA hypermethylation in tumorigenesis: epigenetics joins genetics. Trends Genet 16:168–174

Cohen MM Jr (1999) Overgrowth syndromes: an update. Adv Pediatr 46:441–491

Cole TRP, Hughes HE (1994) Sotos syndrome: a study of the diagnostic criteria and natural history. J Med Genet 31:20–32

Davuluri RV, Grosse I, Zhang MQ (2001) Computational identification of promoters and first exons in the human genome. Nat Genet 29:412–417. DOI 10.1038/ng780

Deardorff MA, Maisenbacher M, Zackai EH (2004) Ganglioglioma in a Sotos syndrome patient with an NSD1 deletion. Am J Med Genet 130A:393–394

de Boer L, Kant SG, Karperien M, van Beers L, Tjon J, Vink GR, van Tol D, Dauwerse H, le Cessie S, Beemer FA, van der Burgt I, Hamel BC, Hennekam RC, Kuhnle U, Mathijssen IB, Veenstra-Knol HE, Stumpel CT, Breuning MH, Wit JM (2004) Genotype–phenotype correlation in patients suspected of having sotos syndrome. Horm Res 62:197–207. DOI 10.1159/000081063

Douglas J, Hanks S, Temple IK, Davies S, Murray A, Upadhyaya M, Tomkins S, Hughes HE, Cole TR, Rahman N (2003) NSD1 mutations are the major cause of Sotos syndrome and occur in some cases of Weaver syndrome but are rare in other overgrowth phenotypes. Am J Hum Genet 72:132–143

Douglas J, Coleman K, Tatton-Brown K, Hughes HE, Temple IK, Cole TR, Rahman N (2005) Evaluation of NSD2 and NSD3 in overgrowth syndromes. Eur J Hum Genet 13:150–153. DOI 10.1038/sj.ejhg.5201298

Harder A, Rosche M, Reuss DE, Holtkamp N, Uhlmann K, Friedrich R, Mautner VF, von Deimling A (2004) Methylation analysis of the neurofibromatosis type 1 (NF1) promoter in peripheral nerve sheath tumours. Eur J Cancer 40:2820–2828

Ioshikhes IP, Zhang MQ (2000) Large-scale human promoter mapping using CpG islands. Nat Genet 26:61–63

Jones PA, Laird PW (1999) Cancer epigenetics comes of age. Nat Genet 21:163–167

Kamimura J, Endo Y, Kurotaki N, Kinoshita A, Miyake N, Shimokawa O, Harada N, Visser R, Ohashi H, Miyakawa K, Gerritsen J, Innes AM, Lagace L, Frydman M, Okamoto N, Puttinger R, Raskin S, Resic B, Culic V, Yoshiura K, Ohta T, Kishino T, Ishikawa M, Niikawa N, Matsumoto N (2003) Identification of eight novel NSD1 mutations in Sotos syndrome. J Med Genet 40:e126

Knudson AG Jr (1971) Mutation and cancer: statistical study of retinoblastoma. Proc Natl Acad Sci USA 68:820–823

Kurotaki N, Imaizumi K, Harada N, Masuno M, Kondoh T, Nagai T, Ohashi H, Naritomi K, Tsukahara M, Makita Y, Sugimoto T, Sonoda T, Hasegawa T, Chinen Y, Tomita HA, Kinoshita A, Mizuguchi T, Yoshiura KI, Ohta T, Kishino T, Fukushima Y, Niikawa N, Matsumoto N (2002) Haploinsufficiency of NSD1 causes Sotos syndrome. Nat Genet 30:365–366. DOI 10.1038/ng863

Kurotaki N, Harada N, Shimokawa O, Miyake N, Kawame H, Uetake K, Makita Y, Kondoh T, Ogata T, Hasegawa T, Nagai T, Ozaki T, Touyama M, Shenhav R, Ohashi H, Medne L, Shiihara T, Ohtsu S, Kato Z, Okamoto N, Nishimoto J, Lev D, Miyoshi Y, Ishikiriyama S, Sonoda T, Sakazume S, Fukushima Y, Kurosawa K, Cheng JF, Yoshiura K, Ohta T, Kishino T, Niikawa N, Matsumoto N (2003) Fifty microdeletions among 112 cases of Sotos syndrome: low copy repeats possibly mediate the common deletion. Hum Mutat 22:378–387

Li LC, Dahiya R (2002) MethPrimer: designing primers for methylation PCRs. Bioinformatics 18:1427–1431

Nagai T, Matsumoto N, Kurotaki N, Harada N, Niikawa N, Ogata T, Imaizumi K, Kurosawa K, Kondoh T, Ohashi H, Tsukahara M, Makita Y, Sugimoto T, Sonoda T, Yokoyama T, Uetake K, Sakazume S, Fukushima Y, Naritomi K (2003) Sotos syndrome and haploinsufficiency of NSD1: clinical features of intragenic mutations and submicroscopic deletions. J Med Genet 40:285–289

Ponger L, Mouchiroud D (2002) CpGProD: identifying CpG islands associated with transcription start sites in large genomic mammalian sequences. Bioinformatics 18:631–633

Rahman N (2005) Mechanisms predisposing to childhood overgrowth and cancer. Curr Opin Genet Dev 15:227–233. DOI 10.1016/j.gde.2005.04.007

Rio M, Clech L, Amiel J, Faivre L, Lyonnet S, Le Merrer M, Odent S, Lacombe D, Edery P, Brauner R, Raoul O, Gosset P, Prieur M, Vekemans M, Munnich A, Colleaux L, Cormier-Daire V (2003) Spectrum of NSD1 mutations in Sotos and Weaver syndromes. J Med Genet 40:436–440

20

Rozen S, Skaletsky H (2000) Primer3 on the WWW for general users and for biologist programmers. Methods Mol Biol 132:365–386

Suter CM, Martin DI, Ward RL (2004) Germline epimutation of MLH1 in individuals with multiple cancers. Nat Genet 36:497–501

Tatton-Brown K, Rahman N (2004) Clinical features of NSD1-positive Sotos syndrome. Clin Dysmorphol 13:199–204

Tatton-Brown K, Douglas J, Coleman K, Baujat G, Cole TR, Das S, Horn D, Hughes HE, Temple IK, Faravelli F, Waggoner D, Turkmen S, Cormier-Daire V, Irrthum A, Rahman N (2005) Genotype–phenotype associations in Sotos syndrome: an analysis of 266 individuals with NSD1 aberrations. Am J Hum Genet 77:193–204

Turkmen S, Gillessen-Kaesbach G, Meinecke P, Albrecht B, Neumann LM, Hesse V, Palanduz S, Balg S, Majewski F, Fuchs S, Zschieschang P, Greiwe M, Mennicke K, Kreuz FR, Dehmel HJ, Rodeck B, Kunze J, Tinschert S, Mundlos S, Horn D (2003) Mutations in NSD1 are responsible for Sotos syndrome, but are not a frequent finding in other overgrowth phenotypes. Eur J Hum Genet 11:858–865. DOI 10.1038/sj.ejhg.5201050

Visser R, Matsumoto N (2003) Genetics of Sotos syndrome. Curr Opin Pediatr 15:598–606

Visser R, Shimokawa O, Harada N, Kinoshita A, Ohta T, Niikawa N, Matsumoto N (2005) Identification of a 3.0-kb major recombination hotspot in patients with sotos syndrome who carry a common 1.9-Mb microdeletion. Am J Hum Genet 76:52–67

ORIGINAL ARTICLE

Takako Ohata · Kunihiro Yoshida · Haruya Sakai
Haruka Hamanoue · Takeshi Mizuguchi
Yusaku Shimizu · Tomomi Okano · Fumio Takada
Kinya Ishikawa · Hidehiro Mizusawa
Ko-ichiro Yoshiura · Yoshimitsu Fukushima
Shu-ichi Ikeda · Naomichi Matsumoto

A −16C>T substitution in the 5′ UTR of the *puratrophin-1* gene is prevalent in autosomal dominant cerebellar ataxia in Nagano

Abstract The molecular bases of autosomal dominant cerebellar ataxia (ADCA) have been increasingly elucidated, but 17–50% of ADCA families still remain genetically undefined in Japan. In this study we investigated 67 genetically undefined ADCA families from the Nagano prefecture, and found that 63 patients from 51 families possessed the −16C>T change in the *puratrophin-1* gene, which was recently found to be pathogenic for 16q22-linked ADCA. Most patients shared a common haplotype around the *puratrophin-1* gene. All patients with the −16C>T change had pure cerebellar ataxia with middle-aged or later onset. Only one patient in a large, −16C>T positive family did not have this change, but still shared a narrowed haplotype with, and was clinically indistinguishable from, the other affected family members. In Nagano, 16q22-linked ADCA appears to be much more prevalent than either SCA6 or dentatorubral-pallidoluysian atrophy (DRPLA), and may explain the high frequency of spinocerebellar ataxia.

Keywords Autosomal dominant cerebellar ataxia · 16q22-linked ADCA · *puratrophin-1* · Nagano

Takako Ohata and Kunihiro Yoshida have equally contributed to this work

T. Ohata · K. Yoshida · H. Sakai · H. Hamanoue
T. Mizuguchi · N. Matsumoto
Department of Human Genetics, Yokohama City University
Graduate School of Medicine, 3-9 Fukuura, Kanazawa-ku,
Yokohama 236-0004, Japan

T. Ohata · F. Takada
Department of Medical Genetics, Kitasato University Graduate
School of Medical Sciences, 1-15-1 Kitasato,
Sagamihara 228-8555, Japan

K. Yoshida (✉) · Y. Shimizu · T. Okano · S. Ikeda
Third Department of Medicine, Shinshu University School
of Medicine, 3-1-1 Asahi, Matsumoto 390-8621, Japan
E-mail: kyoshida@hsp.md.shinshu-u.ac.jp
Tel.: +81-263-372673
Fax: +81-263-373427

K. Yoshida · Y. Fukushima
Division of Clinical and Molecular Genetics, Shinshu University
Hospital, 3-1-1 Asahi, Matsumoto 390-8621, Japan

K. Ishikawa · H. Mizusawa
Department of Neurology and Neurological Science, Graduate
School of Medical and Dental Sciences, Tokyo Medical and Dental
University, 1-5-45 Yushima, Bunkyo-ku, Tokyo 113-8519, Japan

K. Yoshiura
Department of Human Genetics, Nagasaki University Graduate
School of Biomedical Sciences, 1-12-4 Sakamoto,
Nagasaki 852-8523, Japan

Introduction

Autosomal dominant cerebellar ataxia (ADCA) is genetically heterogeneous (Margolis 2003; Schols et al. 2004). The most updated GeneTests (8 November 2005) and HUGO Gene Nomenclature Committee (25 November 2005) cover at least 27 different ADCA subtypes including SCA28. Among these, a coding CAG (or CAA, both coding glutamine) repeat expansion has been found in seven subtypes: SCA1, 2, 3/Machado-Joseph disease (MJD), 6, 7, and 17, and dentatorubral-pallidoluysian atrophy (DRPLA) (Banfi et al. 1994; Kawaguchi et al. 1994; Nagafuchi et al. 1994; Imbert et al. 1996; Pulst et al. 1996; Sanpei et al. 1996; David et al. 1997; Zhuchenko et al. 1997; Koide et al. 1999; Nakamura et al. 2001). A non-coding repeat expansion occurs in three subtypes: SCA8, 10, and 12 (Holmes et al. 1999; Koob et al. 1999; Matsuura et al. 2000; Fujigasaki et al. 2001), and a missense mutation in two of them: SCA14 and 27 (Chen et al. 2003; van Swieten et al. 2003). Several reports regarding 16q22-linked ADCA have been released (Nagaoka et al. 2000; Takashima et al. 2001; Li et al. 2003; Hirano et al. 2004), and a single nucleotide substitution (−16C>T) in the 5′

462

UTR in the *puratrophin-1* gene was recently identified in all patients from 52 unrelated Japanese families sharing a common haplotype at 16q22.1 (Ishikawa et al. 2005).

In Japan, the incidence of spinocerebellar degeneration/ataxia (SCD/SCA) including multiple-system atrophy (MSA) is 15.68 in 100,000. Although SCA6, SCA3/MJD, and DRPLA are the three most prevalent subtypes, their frequencies quite differ from region to region (Maruyama et al. 2002; Sasaki et al. 2003). We previously showed that the incidence of SCA, excluding MSA, was higher (22 in 100,000) in Nagano than in other parts of Japan. In 86 unrelated ADCA families from Nagano, SCA6 (19%) and DRPLA (10%) were common, while SCA3/MJD (3%), SCA1 (2%), and SCA2 (1%) were infrequent (Shimizu et al. 2004). More importantly, the majority of families (65%) were genetically undefined; such families make up 17–50% of the ADCA families in other parts of Japan (Maruyama et al. 2002; Sasaki et al. 2003; Shimizu et al. 2004). A common haplotype of 16q22-linked ADCA reported by Li et al. (2003) was not confirmed in our series (Shimizu et al. 2004).

We hypothesized that there may be distinct ADCA subtypes in Nagano because it is relatively isolated by steep mountains. A genome-wide linkage study was performed in undefined ADCA families to identify possibly new ADCA loci. The −16C > T substitution in *puratrophin-1* was also investigated.

Materials and methods

Subjects

A total of 105 individuals (83 affected and 22 unaffected) from 67 ADCA families originating from the Nagano prefecture were recruited to this study. All affected individuals were examined by at least one experienced neurologist according to the standard clinical criteria. Dominant inheritance was presumed when affected individuals were recognized in at least two generations. Three families (SCAF9, SCAF25, and SCAF41) with several affected members were used for linkage studies. Genomic DNA was isolated from peripheral leukocytes using a PUREGENE DNA purification kit (Gentra Systems, Minneapolis, MN, USA). SCA 1, 2, 3/MJD, 6, 7, 12, and 17, and DRPLA were ruled out after confirming the (CAG)n length by PCR as previously described (Shimizu et al. 2004). This research protocol was approved independently by the Ethical Committee of Shinshu University School of Medicine and by the Committee for Ethical Issues at Yokohama City University School of Medicine.

Linkage analysis

A large family, SCAF41, consisting of 7 affected and 15 unaffected members, was analyzed using 400 polymorphic markers (ABI PRISM Linkage Mapping Set

version 2.5-MD10; Applied Biosystems, Foster City, CA, USA). Furthermore, an additional 21 polymorphic markers mapped to 16q21–16q23.1 (*D16S3111, D16S3050, D16S3021, D16S3043, D16S3019, TAGA02, TTCC01, D16S3086, GATA01, D16S421, TA001, GA001, TTTA001, CATG003, 17msm, D16S3085, D16S3025, CTTT01, D16S3067, GT01,* and *D16S3018*) were used for the study of three families, SCAF9, SCAF25, and SCAF41. Primer sequences are described elsewhere (Hirano et al. 2004; Ishikawa et al. 2005). PCR was cycled 40 times at 94°C for 30 s, 55°C for 30 s, and 72°C for 30 s in a 10-µl mixture containing 10 ng genomic DNA, 0.5 µM of each primer, 0.2 mM each of dNTP, 10× PCR buffer (TaKaRa, Ohtsu, Japan), and 0.25 U of Takara Ex Taq DNA polymerase (TaKaRa). PCR products were analyzed by an ABI 3100 Genetic analyzer (Applied Biosystems), and their product sizes were determined using the GeneMapper Software version 3.5 (Applied Biosystems). Two-point linkage analysis was carried out using the LINKAGE Program Package (FASTLINK software, version 5.1). The allele frequencies of the markers were set as equal when they were unknown. The disease gene frequency was assumed to be 0.00001. The possibly affected individuals were scored as unknown. LOD scores were corrected by age-dependent penetrance established based on the cumulative age at onset (penetrance 0 for persons aged 39 years and younger, 0.08 for those aged 40–49 years, 0.37 for those aged 50–59 years, 0.79 for those aged 60–69 years, and 0.99 for those aged 70 years or older).

Analysis of a single nucleotide substitution (−16C > T) in the 5′ UTR of *puratrophin-1*

Primer sequences have been described elsewhere (Ishikawa et al. 2005). PCR was cycled 35 times at 94°C for 30 s, 65°C for 30 s, and 72°C for 30 s in a 20-µl mixture containing 30 ng genomic DNA, 0.5 µM of each primer, 0.2 mM each of dNTP, 10× PCR buffer (TaKaRa), and 0.25 U of Takara Ex Taq DNA polymerase (TaKaRa). PCR products were purified with ExoSAP-IT (USB, Cleveland, OH, USA) and sequenced by a standard protocol using BigDye terminator (Applied Biosystems) on an ABI PRISM 3100 Genetic analyzer (Applied Biosystems). Nucleotide substitution was confirmed using the SeqScape software version 2.0 (Applied Biosystems), and by *Eco*NI RFLP designed by Ishikawa et al. (2005). All patients were genotyped for at least nine markers: *16S3086, GATA01, D16S421, TA001, GA001, TTTA001, CATG003, 17msm,* and *D16S3085,* to confirm haplotypes.

Results

Genome-wide linkage analysis using 400 markers in SCAF41 did not give any locations of maximum LOD scores of three or more. Although several locations with

relatively high scores were identified, including *D1S2785* on 1q43 (LOD, 1.18 [$\theta=0$]), *D8S549* on 8p22 (LOD, 1.43 [$\theta=0$]), *D16S515* on 16q23.1 (LOD, 1.03 [$\theta=0$]); thus, the initial screening failed to reveal a specific locus for the disease.

During this study, the single nucleotide substitution (−16C > T) in the 5′ UTR of the *puratrophin-1* gene was identified as a possible pathological change for 16q22-linked ADCA (Ishikawa et al. 2005). We found this substitution in 11 out of 12 affected and 2 out of 22 unaffected individuals in SCAF9, SCAF25, SCAF41 (Fig. 1), and 16q22-focused linkage analysis in these three families using additional 21 markers gave a maximum LOD score at *TAGA02* of 2.42 ($\theta=0$). Haplotype analysis demonstrated a common haplotype (1-3-2-T-1-2-5-1-2-2 at *D16S3086 −GATA01 −D16S421 −* [−16C/T of *puratrophin-1* {*Q9H7K4*}] *−TA001 −GA001 −TTTA001 −CATG003 −17msm −D16S3085*) in all affected members except SCAF41-21 and two young unaffected members, SCAF41-10 (40 years old) and SCAF25-5 (41 years old), who may be obligate carriers. It is noteworthy that SCAF41-21 (59 years old) did not have the −16C > T change, but shared only a narrowed

haplotype (1-3-2 at *D16S3086 −GATA01 −D16S421*) as it is assumed that a recombination happened between *D16S421* and *Q9H7K4*. While her clinical symptoms were still mild, a slowly progressive gait ataxia and clumsiness in the hands were evident.

Further analysis of nine markers (*D16S3086*, *GATA01*, *D16S421*, *TA001*, *GA001*, *TTTA001*, *CATG003*, *17msm*, and *D16S3085*), as well as the −16C > T change, was performed in the other 71 patients from 64 families (Fig. 2). We found that 53 patients from 48 families carried the −16C > T substitution and their phenotypes were compatible with pure cerebellar ataxia. Their average age of disease onset was 60.2 ± 9.3 years (mean ± 1 SD), while the average age of onset for 18 patients from 16 families without the substitution was 37.9 ± 20.8 years and most of them showed juvenile-onset cerebellar ataxia, or extracerebellar neurological symptoms such as parkinsonism, dementia, and/or involuntary movements. Genetic anticipation was observed in two families. Five out of 16 families without the −16C > T change showed late-onset, pure cerebellar ataxia indistinguishable from that of typical patients with the −16C > T change in the *pura-*
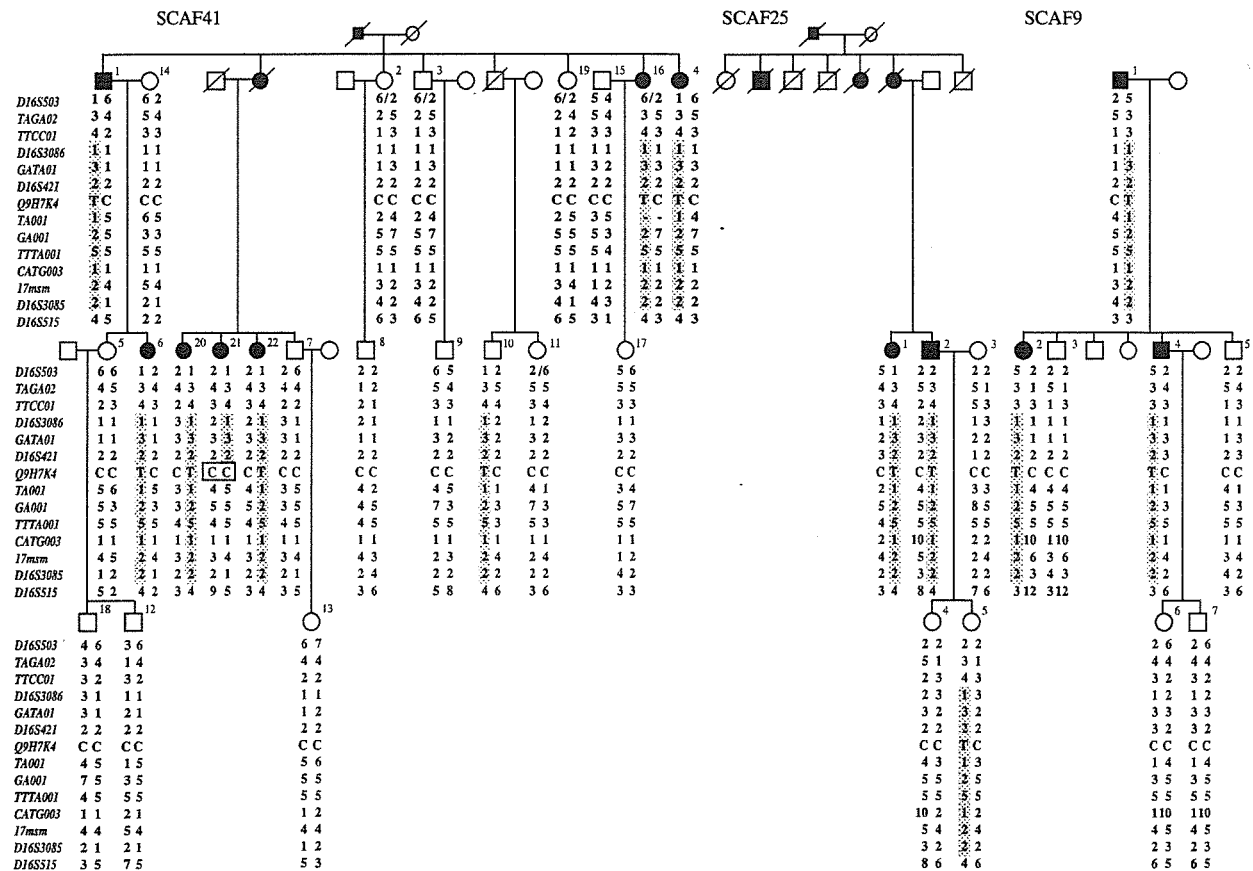
Fig. 1 Haplotype analysis in three large ADCA families, SCAF41, SCAF25, and SCAF9. Thirteen polymorphic markers mapped to 16q21–16q23 and the −16C > T substitution in *puratrophin-1* (*Q9K7H4*) are shown. Twelve affected and two unaffected individuals had a common haplotype (1-3-2) at *D16S3086–GATA01–D16S421*. The −16C > T substitution was found in 11 out of 12 affected and 2 out of 22 unaffected individuals

464

A: Patients with -16C>T substitution

B: Patients without -16C>T substitution

Fig. 2 Genotype of 71 patients from the other 64 families. The −16C>T substitutions in *puratrophin-1* (*Q9K7H4*) was observed in 53 patients from 48 families (**A**), but not in 18 patients from 16 families (**B**). A haplotype, 2-1-2-5-1-2-2 of seven markers (*D16S421 −TA001 −GA001 −TTTA001 −CATG003 −17msm−D16S3085*) was shared by 50 patients with the −16C>T change and another haplotype, 2-6/14-2-5-1-2-2 for the same markers was shared by three patients (patient IDs, 45, 64, and 71). *N* unknown

trophin-1 gene. Additionally, four negative controls, SCA6 patients, also did not have the −16C>T change (data not shown). Among the 51 families with the −16C>T change, 49 of them shared a common haplotype around the *puratrophin-1* gene, 2-1-2-5-1-2-2 for seven markers (*D16S421 −TA001 −GA001 −TTTA001 −CATG003 −17msm −D16S3085*), and two families showed a slightly different haplotype, 2-6/14-2-5-1-2-2.

Discussion

The −16C>T change in the 5′ UTR of *puratrophin-1* was found in 51 out of 67 ADCA families (76%) from the Nagano prefecture, in which SCA1, 2, 3/MJD, 6, 7, 12, 17, and DRPLA had been previously ruled out. Among 106 ADCA families genetically analyzed to date (unpublished observation), the frequency of 16q22-linked ADCA (51 out of 106, 48%) is much higher than that of either SCA6 (18 out of 106, 17%) or DRPLA (9 out of 106, 8%). Thus, an accumulation of 16q22-linked ADCA families leads to a high prevalence of SCD in Nagano. Almost all patients shared the haplotype 2-1-2-5-1-2-2 for markers *D16S421 −TA001 −GA001 −TTTA001 −CATG003 −17msm −D16S3085*. For five of these markers, *D16S421 −TA001 −GA001 −TTTA001 −CATG003*, our haplotype 2-1-2-5-1 was identical to the haplotype 3-1-4-4-4 reported by Ishikawa et al. (2005), based on the data of four patients from two families that

were analyzed independently by both groups. Sixty-four patients from 51 families with the −16C>T substitution showed pure cerebellar ataxia with middle-aged or later onset (Harding's ADCAIII; Harding 1993), while most of the patients without the substitution showed clinical phenotypes characterized by juvenile-onset cerebellar ataxia, additional extracerebellar neurological symptoms, and/or genetic anticipation. Previously, we could not confirm the common haplotype of 16q22-linked ataxia reported by Li et al. (2003; Shimizu et al. 2004), being inconsistent with the current data. This is partly explained by the fact that the focused region presented here was much narrower than the previously haplotyped region.

The −16C>T substitution in the 5′ UTR of *puratrophin-1*, a region of the gene presumed to be regulatory, is unique as a disease-causing change for ADCA. To date, pathological single nucleotide substitutions have been found only in SCA14 or SCA27 (Chen et al. 2003; van Swieten et al. 2003), both of which are missense mutations. It has been speculated that the −16C>T change might decrease mRNA expression of *puratrophin-1*, and cause aggregation of puratrophin-1 protein in Purkinje cells in affected cerebellum (Ishikawa et al. 2005).

Ishikawa et al. (2005) found the −16C > T substitution in the *puratrophin-1* gene in all affected individuals from 52 unrelated Japanese families. However, in this study there was one exceptional patient without this substitu-